arXiv:cond-mat/0606697v2 [cond-mat.stat-mech] 28 Aug 2006

Fermionic atoms trapped in one-dimensional optical superlattice with harmonic confinement

Takanori Yamashita and Norio Kawakami
Department of Applied Physics, Osaka University, Suita, Osaka 565-0871, Japan

Makoto Yamashita
NTT Basic Research Laboratories, NTT Corporation, 3-1, Morinosato-Wakamiya, Atsugi-shi, Kanagawa 243-0198, Japan

(Dated: March 23, 2022)

We study the ground-state properties of spin-1/2 fermionic atoms confined in a one-dimensional optical superlattice with harmonic confinement by using the density matrix renormalization group method. For this purpose, we consider an ionic Hubbard model that has superlattice potentials with 2-site periodicity. We find that several different types of insulating regimes coexist even if the number of atoms at each site is not an integer, but its average within the unit cell is an integer or half integer. This is contrasted to the coexisting phase of the metallic and Mott-insulating regimes known for the ordinary Hubbard model in an optical lattice. The phase characteristics are elucidated by investigating the profiles of the atom density, the local density/spin fluctuations, the double occupation probability and the spin correlations in detail.

PACS numbers: 03.75.Ss, 05.30.Fk, 34.50.-s, 71.30.+h

I. INTRODUCTION

Experimental techniques for manipulating ultracold atoms have made great progress since the successful realization of atomic Bose-Einstein condensates (BECs) [1]. Optical lattices, formed by a standing wave of laser light, are providing the ideal stages for an experimental investigation of the fundamental many-body problems in condensed matter physics via ultracold atomic gases [2, 3, 4, 5]. A recent series of experimental studies on bosonic Mott-insulators [6, 7, 8, 9, 10, 11, 12] have clearly demonstrated this feature, namely the realization of quantum simulators.

A noteworthy advantage of atomic gases over condensed matter such as solids or liquids is that their experimental parameters are highly controllable. Both density and temperature of atomic gases are fully controlled in the process of evaporative cooling [1]. The depth of the optical lattice potential is controlled by the light intensity, which leads to the precise alternation of atom tunneling between adjacent sites [2, 3]. Furthermore, we can create one-, two-, and three-dimensional optical lattices depending on the laser beam configuration with the use of interference effects [2, 3]. Even the interactions between the atoms can be widely tuned with the help of Feshbach resonances [13]. Therefore, in the experiments, it is possible to precisely change the important system parameters such as density, temperature, tunneling, dimensionality of lattices, interaction strength and so forth. Ultracold atoms in optical lattices allow us to investigate the quantum many-body effects in a well-controlled manner.

Experiments with quantum degenerate fermionic gases have already clarified the intriguing physics of such phenomena as a molecular BEC [14, 15, 16] and the crossover between a BEC and a Bardeen-Cooper-Schrieffer (BCS) superfluid [17, 18, 19, 20]. Ultracold fermionic atoms trapped in optical lattices are now stimulating both experimental and theoretical interest. This system is well captured by the Hubbard model Hamiltonian [21], which is widely discussed with respect to strongly correlated electron systems. Several theoretical analyses have predicted the possibility of the Mott metal-insulator transition (MMIT) in this system [21, 22, 23, 24, 25, 26]. Although experimental investigations are still under way [27, 28, 29, 30], the recent demonstration of a fermionic band insulator in three-dimensional optical lattices [29] has convinced us that MMIT will be observed in near future. A precise comparison of the theory and experiments will provide us with a deeper understanding of the quantum phase transition in fermionic systems.

The *superlattice* geometry of optical lattices, i.e., optical superlattice, was successfully demonstrated as an advanced manipulation technique in a recent report [31]. This technique has been introduced to control the distribution of atoms on lattices more functionally and will play a key role in the implementation of quantum computing with ultracold atoms [4, 31]. On the other hand, in condensed matter physics, it is known that lattice distortions generate a variety of many-body effects in strongly correlated electron systems such as the charge-transfer organic materials and ferroelectric perovskites [32, 33, 34, 35, 36, 37, 38, 39, 40, 41, 42, 43, 44, 45, 46]. The ultracold fermionic atoms in optical superlattices [47] can be regarded as a quantum simulator for these materials. Our present study is highly motivated by these important potentialities of optical superlattices.

In this paper, we investigate the ground state properties of S=1/2 fermions trapped in a one-dimensional optical superlattice with 2-site periodicity. The external harmonic confinement inherent in the real experiments [2] is further considered in our model. We show that a

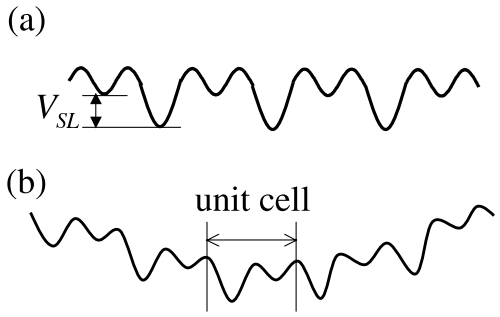


FIG. 1: Potential profiles of (a) 2-site periodic superlattice and (b) with a confining potential. V_{SL} is the difference between the potential energies of odd and even sites.

new coexistence phase appears consisting of three distinct insulating regions caused by the superlattice potentials, which is in contrast to the ordinary Hubbard model in the optical lattice. This is elucidated via a detailed analysis of the local density of atoms and spin correlations by using the density matrix renormalization group method. Furthermore, we find unique spin correlations between the insulating regions when these regions are separated by a metallic region.

This paper is organized as follows. In the next section we briefly mention the model and the method. We then show the density profiles of fermions and several density/spin correlation functions to clarify the zero temperature properties. The final section provides a brief summary.

II. MODEL AND METHOD

We consider a gas of fermionic atoms embedded in an optical superlattice with an alternating superlattice potential and a confining parabolic potential (see Fig. 1(b)), which is described by the Hubbard Hamiltonian,

$$\begin{aligned}\mathcal{H} &= -t\sum_{i,\sigma}(c^{\dagger}_{i,\sigma}c_{i+1,\sigma}+h.c.)+U\sum_{i}n_{i\uparrow}n_{i\downarrow}\\ &+\sum_{i,\sigma}V_i n_{i\sigma}+V_c\sum_{i\sigma}(i-N_s/2)^2 n_{i\sigma} \qquad (1)\end{aligned}$$

where $c^{\dagger}_{i\sigma}$, $c_{i\sigma}$ and $n_{i\sigma}=c^{\dagger}_{i\sigma}c_{i\sigma}$ are respectively the fermion creation, annihilation and number operators relevant to the site labeled i with spin $\sigma(=\uparrow,\downarrow)$. Here, U is the on-site repulsion ($U>0$), V_c the curvature of the parabolic confining potential, V_i the local potential at site i and t the hopping amplitude between nearest neighbor sites.

We define the local potential V_i with 2-site periodicity as

$$V_i = V_{SL}\{\mathrm{mod}(i+1,2)\} \qquad (2)$$

where V_{SL} is the difference between the potential energies of odd and even sites (see Fig. 1(a)). We denote the total number of fermions (lattice sites) as N_f (N_s).

There are several kinds of numerical methods that can be employed with our fermionic superlattice Hubbard model. The numerical diagonalization method can be applied straightforwardly to fermionic models, but it restricts our analysis to rather small systems with a typical lattice size of 20 sites, which is not large enough for our purpose. The quantum Monte Carlo simulations method is an efficient way to deal with quantum systems at finite temperatures, and this approach has been applied successfully to bosonic Hubbard models to elucidate the transition between the superfluid and Mott insulating phases in optical lattices [48, 49, 50]. This method, however, suffers from negative-sign problems in fermionic cases, which makes it difficult to obtain reliable results at low temperatures. The density matrix renormalization group (DMRG)[51, 52] is another powerful numerical method with which we investigate quantum systems such as fermionic models with extremely high accuracy, although it is restricted to one-dimensional cases. This technique allows us to deal with a very large system as required for the analysis of optical lattices. In this paper we therefore exploit a variant of the DMRG (the so-called finite-system DMRG) [51] to study our fermionic Hubbard model in an optical superlattice at zero temperature. The essence of the idea is that we first diagonalize a given small system, and then enlarge the system size step by step via a renormalization procedure by retaining relevant low-energy states which have large eigenvalues of the density matrix. This simple procedure is known to give precise results for one-dimensional quantum systems. This method has already been reported in detail [51, 52]. In our nonuniform model with harmonic confinement, the numerical calculation can be done in parallel to the ordinary case without confinement. The only point we have to pay attention to is that the superlattice potential should be properly included in each renormalization step.

We restrict our discussions to the singlet ground state with an even number of fermions, which are tractable by the DMRG method [51, 52]. As far as the local density and its variance are concerned (see Sec.III A and B), the even-number case is sufficient to discuss the characteristic properties. A relevant difference between the even and odd cases may appear in the spin correlations (Sec.III C) since a free S=1/2 spin remains unscreened in the system for the odd case. The free spin is not important physically since it does not affect the global nature of the system, but rather acts as a magnetic impurity.

III. RESULTS

A. Density profiles

In our optical lattice, the spatial distribution of atoms is inhomogeneous because of the confining harmonic po-

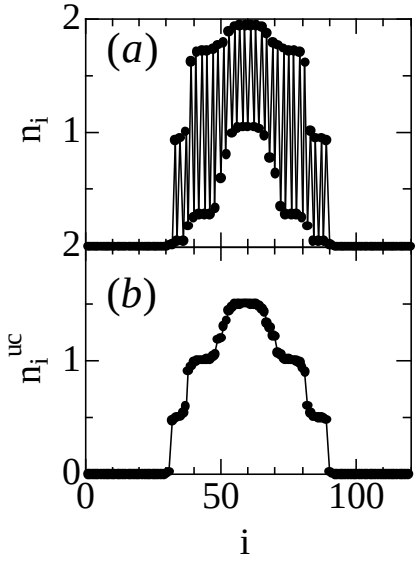


FIG. 2: (a) Density profiles for a trap with $N_s = 120$, $N_f = 60$, $V_c/t = 0.01$, $U/t = 4.0$ and $V_{SL}/t = 6.0$. The filled circles denote the local density n_i and the solid lines are a guide for the eye. (b) shows the density profile, n_i^{uc}, averaged within the unit cell. There are plateaus at $n_i^{uc} = 0.5, 1.0$, and 1.5.

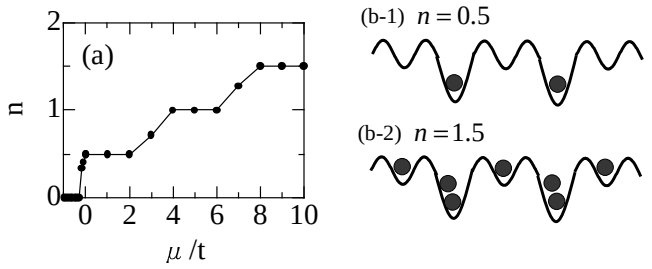


FIG. 3: Metallic and insulating phases in the one-dimensional homogeneous superlattice system without harmonic confinement for $V_{SL}/t = 6.0$ and $U/t = 4.0$: (a) density of atoms, n, as a function of the chemical potential μ/t. The plateaus, which are formed clearly at n=0.5, 1.0, and 1.5, imply the existence of well-defined insulating phases. (b-1) and (b-2) are schematic diagrams of the insulating phases for $n = 0.5$ and 1.5.

tential. We thus consider the profile of the local density, i.e. the spatial distribution of n_i, to be

$$n_i \equiv \sum_\sigma \langle c_{i\sigma}^\dagger c_{i\sigma} \rangle. \tag{3}$$

In Fig. 2(a), we show the density profile for $N_f = 60$ fermions trapped in a lattice with the linear size $N_s = 120$, where the other parameters are $V_{SL}/t = 6.0$, $U/t = 4.0$ and $V_c/t = 0.01$. It is seen in Fig. 2(a) that the amplitude of the local density alternates between even and odd sites reflecting the 2-site periodic potential. When there is no superlattice structure, namely V_{SL}=0, it is known that a Mott insulating region appears characterized by plateau formation at $n_i = 1.0$ [21, 22]. In the present case, however, the density profile reveals more complicated sawtoothed structures, from which we can not immediately distinguish metallic and insulating regions. To characterize the insulating region clearly, we therefore introduce the average number of atoms in the unit cell as,

$$n_i^{uc} \equiv \frac{1}{2}(n_i + n_{i+1}). \tag{4}$$

In Fig. 2(b), we show the n_i^{uc} value obtained by averaging the data of (a) in the unit cell. Plateaus (or shoulders) appear at n_i^{uc} =0.5, 1.0, and 1.5, which characterize three distinct insulating regions.

To understand the above characteristic behavior in n_i^{uc}, it is instructive to observe the bulk properties of the system without harmonic confinement, which are shown in Fig. 3. Figure 3(a) shows the infinite DMRG results for filling factor n as a function of chemical potential μ. We can see the formation of well-defined plateaus at n =0.5, 1.0, and 1.5, which clearly feature the insulating phases separated by the metallic phases. The insulating phases with n =0.5 and 1.5 are caused by the superlattice potential with 2-site periodicity. The corresponding spatial distribution of atoms is schematically illustrated in Fig. 3(b). When $n = 0.5$, as shown in Fig. 3(b-1), the system is in a variant of the Mott insulating phase where each site with lower (higher) potential V_i accommodates one (no) atom. On the other hand, when $n = 1.5$, as shown in Fig. 3(b-2), the system is another Mott type insulator where each site with higher potential accommodates one atom, while that with lower potential is almost fully occupied by two atoms. The insulating phase with $n = 1.0$ changes its nature depending on the interaction strength U in a slightly complicated way, from the band insulator (small U) to the Mott insulator (large U). Actually this problem has been extensively discussed so far, which is briefly summarized here. Early studies by the numerical [36] and weak-coupling bosonization methods [37] suggested that a single phase transition occurs from the band insulator to the Mott insulator when U is varied at half filling. On the other hand, Fabrizio *et al.* predicted a new intermediate insulating phase "so-called bond-charge density wave (BCDW) phase" between them [38]. Since their proposal, extensive investigations have been done to confirm it. Quantum Monte Carlo simulations [39] supported the existence of the intermediate phase. By applying the method of topological transitions in spin and charge Berry phases, Torio *et al.* presented a ground-state phase diagram, which is consistent with the scenario of Fabrizio *et al.* [40] The DMRG calculations [41, 42, 43, 44] have been performed by several groups. For example, the calculation of various structure factors supported the existence of intermediate phase [43] though Kampf *et al.* [44] were not able to resolve two transitions clearly. Recent calculations based on the DMRG [45] and the level-spectroscopy method [46] with high accuracy have confirmed the existence of the intermediate

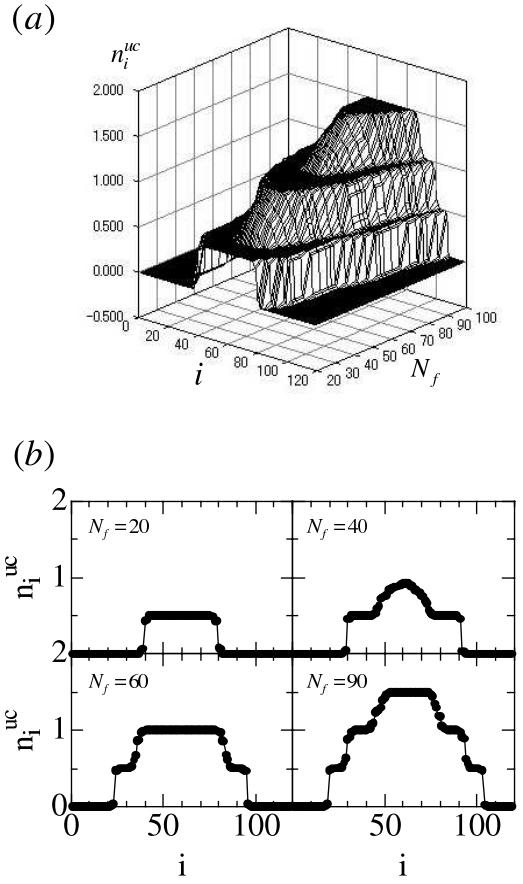


FIG. 4: (a) Profiles of the average density, n_i^{uc}, along the trap for different fillings. The flat terraces are the insulating regions. The parameters are $N_s = 120$, $U/t = 4.0$, $V_{SL}/t = 6.0$, and $V_c/t = 0.005$. In (a), the number of atoms is changed from 20 to 104, while in (b) the number is fixed as N_f =20, 40, 60, and 90.

BCDW phase.

The above results for the homogeneous system show that the plateau regions at n_i^{uc} =0.5, 1.0, and 1.5 in the system with confining potential have the above insulating properties, which are sandwiched by metallic regions.

Let us now observe how the density profile of the system changes when the atom number N_f is changed systematically. In Fig. 4(a), we show the average density of atoms, n_i^{uc}, when N_f is changed continuously. It is seen that the system enters several distinct ground states as N_f increases. In Fig. 4(b), for reference, we show cross-sectional views of (a) by selecting several typical N_f values. For $N_f = 20$, there is an insulating region with $n_i^{uc} = 0.5$ in the middle of the system. Just bedside this region, there are narrow metallic region windows with $n_i^{uc} < 0.5$, which smoothly continue to the vacant-atom region $n_i^{uc} \sim 0$. The system is therefore in a phase where metals and insulators coexist, as is the case for an ordinary optical lattice without superlattice potentials [21, 22]. For $N_f = 40$, a metallic region with $0.5 < n_i^{uc} < 1.0$ appears in the middle of the system, so that the insulating regions with $n_i^{uc} = 0.5$ are now sandwiched by the two metallic regions with $n_i^{uc} < 0.5$ and $0.5 < n_i^{uc} < 1.0$. For $N_f = 60$, another insulating phase with $n_i^{uc} = 1.0$ emerges in the middle region, and a further increase in the atom number, as seen when $N_f = 90$, results in an insulating region where $n_i^{uc} = 1.5$.

A brief comment on the finite-size effect is in order here. Since we are dealing with the rather small system with 60 fermions, the resulting metallic regions are very narrow, and the density profile changes very sharply there. This is due to the finite-size effect of our small system. If we consider a system with larger number of fermions, the metallic regions become wider and the density profile changes more smoothly.

B. Density fluctuations

In order to characterize the above insulating regions, we further investigate local density fluctuations in our superlattice system. To this end, we introduce the variance of local density fluctuations, Δ_i, at each site as

$$\Delta_i \equiv \langle n_i^2 \rangle - \langle n_i \rangle^2. \tag{5}$$

In ordinary one-dimensional optical lattices, it is known that Δ_i is suppressed and forms a plateau in the insulating region, while it has larger values in the metallic region [21, 22]. This quantity, therefore, can describe the way in which insulator-metal crossover occurs when the on-site repulsion increases.

Figure 5 shows the local density n_i, the average density n_i^{uc}, the variance Δ_i and the double-occupation probability $\langle n_{i\uparrow} n_{i\downarrow} \rangle$ for three different choices of U/t with the other parameters unchanged.

It is convenient to discuss characteristic properties by specifying each region in terms of the average local density n_i^{uc}. Let us first observe the insulating region characterized by $n_i^{uc} = 1.0$, which is located around the site $i = 45$ (or equivalently $i = 75$) in all three cases in Fig. 5. For $U/t = 0.0$, we can see the sawtoothed oscillation both in n_i and $\langle n_{i\uparrow} n_{i\downarrow} \rangle$ since the system is in the band insulator where almost doubly-occupied sites and vacant sites are realized alternately. Note that even in this case, the variance Δ_i forms a plateau without such alternations, implying that density fluctuations occur locally only via a process between two adjacent sites. As the interaction strength U increases, n_i ($\langle n_{i\uparrow} n_{i\downarrow} \rangle$) continuously approaches $n_i \to 1$ ($\langle n_{i\uparrow} n_{i\downarrow} \rangle \to 0$). On the other hand, Δ_i is once enhanced ($U/t = 3.0$, Fig. 5(b)), and then suppressed ($U/t = 9.0$, Fig. 5(c)). Therefore, we naturally expect that there may be another insulating state, which is characterized by an enhanced Δ_i, between the band insulating state (small U) and the Mott insulating state (large U). As mentioned above, in a homogeneous system without confinement, at half filling (corresponding to $n_i^{uc} = 1.0$), the BCDW intermediate phase appears between the band-insulating phase and the Mott insulating phase [38, 39, 40, 41, 42, 43, 44, 45, 46]. In the

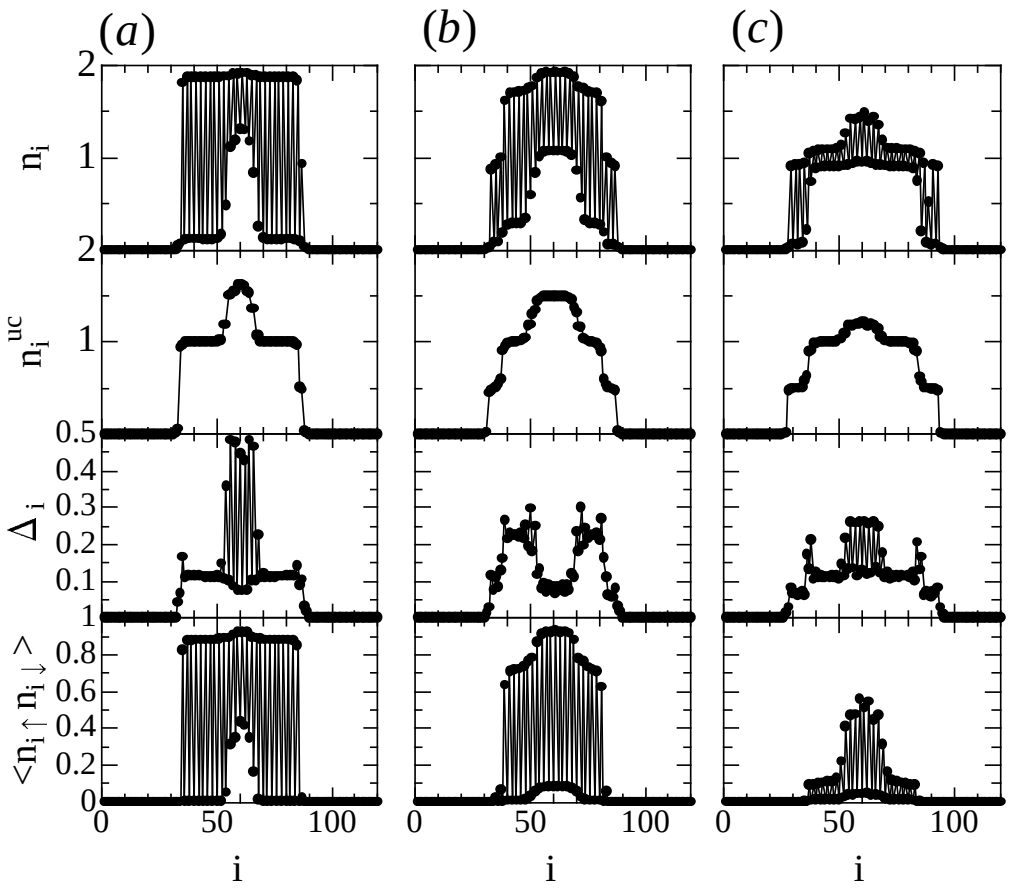


FIG. 5: Plots of the local density n_i, the average density n_i^{uc}, the variance Δ_i and the double-occupation probability $\langle n_{i\uparrow} n_{i\downarrow} \rangle$ for (a) $U/t = 0.0$, (b) 3.0, and (c) 9.0. The other parameters are fixed as $N_f = 60$, $N_s = 120$, $V_c/t = 0.01$, and $V_{SL}/t = 5.0$.

BCDW state, there is rather large hopping within a coupled dimer, which gives rise to enhanced local density fluctuations. Therefore, we can distinguish the BCDW state from the other insulating states in terms of the variance Δ_i. Summarizing the above results, we can say that the region with $n_i^{uc} = 1.0$ is either in the band insulating state, the BCDW state or the Mott insulating state depending on the strength of the on-site repulsion. These states are smoothly connected to each other with the increase in U (crossover behavior) in contrast to the phase transitions realized in the homogeneous case.

We next focus on the region around the site $i = 35$, where the average density $n_i^{uc} = 1.0$ at $U/t = 0.0$ is changed to $n_i^{uc} = 0.5$ at $U/t = 3.0$ and 9.0. In this case, the local density n_i is reduced from 2 to 1 at each odd site with the increase in U, and Δ_i and $\langle n_{i\uparrow} n_{i\downarrow} \rangle$ decrease monotonically to zero (even sites are always empty). Namely, the system is smoothly driven from the band insulator to the Mott insulator. Finally, we look at the region around $i = 60$, where n_i^{uc} is slightly larger than 1.5 at $U/t = 0.0$ without plateau structures, which is characteristic of the metallic region. In fact, Δ_i exhibits strong even-odd dependence on the site index. At $U/t = 3.0$, we see the plateau formation at $n_i^{uc} = 1.5$, where $n_i \sim 1.0$ and $\langle n_{i\uparrow} n_{i\downarrow} \rangle \sim 0$ for even sites. Therefore, the region enters the insulating region with Mott (odd sites) and band-insulating (even sites) characteristics. A further increase in U again drives the Mott insulating state to the metallic state characterized by $1.0 < n_i^{uc} < 1.5$.

We have repeated similar calculations for various choices of the model parameters. Among them we have presented only the three selected cases above, since they capture most of the essential properties realized in our optical superlattice with 2-site periodicity.

C. Spin correlations

Finally, we discuss local and spatially-extended spin correlations in the system. In Fig. 6(a)-(c), we show the computed results for the variance of local spin fluctuations $\Delta S_i = \langle (S_i^z)^2 \rangle$ together with the density profile n_i and the average profile n_i^{uc} for the system with $V_{SL}/t = 5.0$ and $U/t = 5.0$. Also shown in Fig. 7(a)-(c) is the spin correlation function $\langle S_i^z S_j^z \rangle$ between the

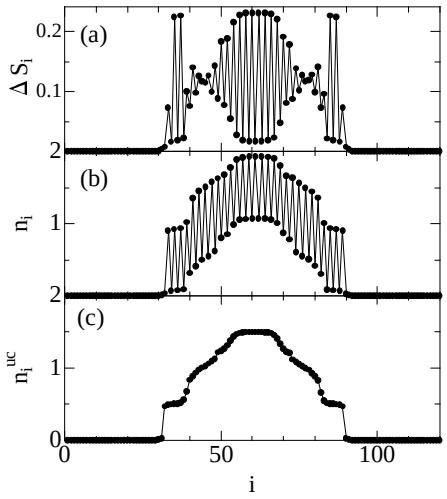


FIG. 6: Plots of (a) the variance of local spin fluctuations ΔS_i together with (b) n_i and (c) n_i^{uc}. The data are obtained for the system with $V_{SL}/t = 5.0$, $U/t = 5.0$. The other parameters are fixed as $N_s = 120$, $N_f = 60$, $V_c/t = 0.01$.

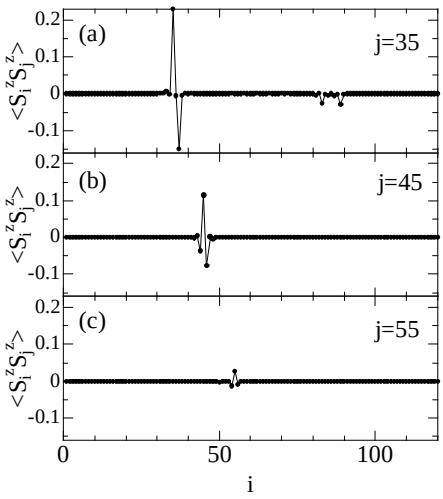


FIG. 7: Plots of the spin correlation function between the ith and jth sites, $\langle S_i^z S_j^z \rangle$, where the site j is fixed as (a)$j = 35$, (b)45 and (c)55. The data are obtained for the system with $V_{SL}/t = 5.0$, $U/t = 5.0$. The other parameters are fixed as $N_s = 120$, $N_f = 60$, $V_c/t = 0.01$.

ith and jth sites with the latter fixed as three typical positions, $j = 35$, 45, and 55.

As clearly seen from Fig. 6, the local moment is well developed ($\Delta S_i > 0.2$) when a given site is located in the Mott insulating region, while it is suppressed ($\Delta S_i \sim 0$) in the band-insulating region as well as in the empty region. These characteristic properties are in accordance with what we naively expect from the homogeneous case without harmonic confinement. Let us now look briefly at the spin correlation function.

In Fig. 7(a), the i-dependence of the spin correlation $\langle S_i^z S_j^z \rangle$ is shown where the site $j = 35$ is fixed in the insulating region with $n_i^{uc} = 0.5$. It is seen that the spin correlation exhibits an antiferromagnetic nature within the same region, and quickly decays when the site i enters the metallic region. Interestingly, the spin correlation increases slightly again around $i = 85$ belonging to another insulating region with $n_i^{uc} = 0.5$. This unusual behavior is discussed below in detail by using a more significant example. On the other hand, for $j = 45$ in the insulating region with $n_i^{uc} = 1.0$, we cannot see the long-range spin correlation as in the $j = 35$ case, since this Mott insulating region is not well stabilized as regards the choice of parameters. For $j = 55$ in Fig. 7(c), the spin correlation shows typical behavior inherent in the metallic state: a small spin correlation amplitude, which immediately decreases with distance.

In Figs. 8 and 9, we show the results obtained when we chose a slightly larger interaction strength U. In this case also, the spin correlation shows similar behavior to that in Fig. 7. There are two points to be mentioned here. Since in this case the local moment is well developed in the Mott insulating region, as seen from Fig. 8(a), the spin correlation shows more significant antiferromagnetic correlations. Even for site j belonging to the metallic region, we can observe slightly enhanced antiferromagnetic correlations (Fig. 9(c)). Another important point to be noticed is that the spin correlations in Fig. 9(a) are strongly enhanced around $i = 85$, although they are suppressed in the region of $i < 85$ (c.f. Fig. 7(a)). This characteristic behavior is a new feature that has not been observed in homogeneous systems without confinement. This is closely related to the formation of several distinct regions. In the Mott insulating region, a finite number of local spins are well developed, which are sensitive to effective magnetic fields. Such spins belonging to the different Mott regions can have enhanced correlations even if they are separated by the metallic phases. This is why we have encountered enhanced spin correlations between $j = 35$ and $i = 85$ in Fig. 9(a). It should be noted that this effect is particularly significant if there is an odd number of spins in the Mott region. For example, in Figs. 7(a) and 9(a), 3 sites around $j = 35$ and $i = 85$ belong to the well-defined Mott regions, which indeed exhibit enhanced spin correlations.

Therefore, the above phenomenon is related to the finite-size effect of the Mott region, so that such behavior should be somewhat obscured when the Mott regions become large. It is thus interesting to know whether such behavior can really be observed by future experiments in the optical lattices.

IV. SUMMARY

We have studied the characteristic properties of fermions trapped in a one-dimensional optical superlattice with 2-site periodicity. We found that plateau re-

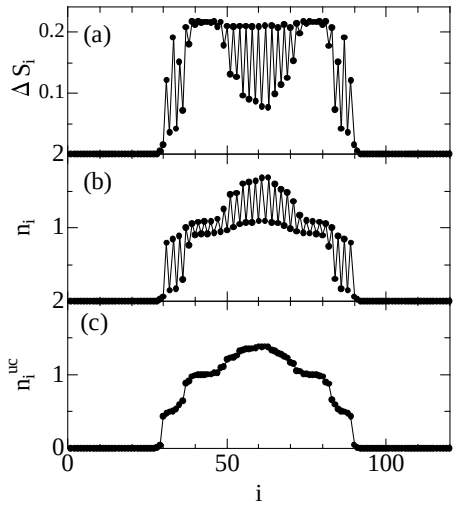


FIG. 8: Similar plots to those in Fig.6 for the other choice of $V_{SL}/t = 3.0$ and $U/t = 7.0$.

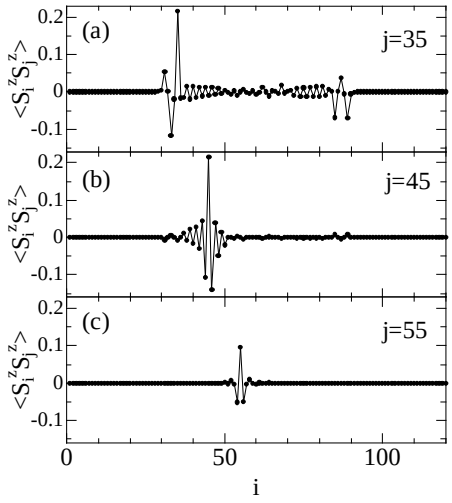


FIG. 9: Similar plots to those in Fig.7 for the other choice of $V_{SL}/t = 3.0$ and $U/t = 7.0$.

gions appear in the profiles of the average number of atoms in the unit cell n_i^{uc}=0.5, 1.0, and 1.5. In contrast to the ordinary Hubbard model in the optical lattice, new insulating regions appear with n_i^{uc} =0.5 and 1.5 caused by the superlattice potentials. Furthermore, it has been shown by the variance and double-occupation probability results that three different insulating regions of band-, BCDW- and Mott-type emerge in the insulating region with $n_i^{uc} = 1.0$, which are smoothly connected to each other via a crossover as the strength of the on-site repulsion U is altered.

We have also found that it is possible to enhance spin correlations between different Mott regions, even if they are once suppressed in the intermediate metallic region. This interesting phenomenon is due to the finite-size effect of the insulating regions, which are naturally formed by harmonic confinement. Specifically, it occurs more significantly when an effective number of sites in the Mott insulating region is odd.

Since systematic experimental studies on the one-dimensional optical superlattice may be soon within our reach, we hope that the characteristic properties discussed for cold fermions in this paper will be observed in the near future.

Acknowledgments

The numerical computations were carried out at the Supercomputer Center, the Institute for Solid State Physics, University of Tokyo. This work was supported by Grant-in-Aid for Scientific Research on Priority Areas (Grant No. 18043017) from The Ministry of Education, Culture, Sports, Science and Technology of Japan.

[1] For a review, see Nature (London) **416**, 205-246 (2002).
[2] I. Bloch and M. Greiner, in *Advances in Atomic, Molecular, and Optical Physics*, editied by P. Berman and C. Lin (Academic Press, New York, 2005), Vol. 52, p. 1.
[3] I. Bloch, Nature Phys. **1**, 23 (2005).
[4] D. Jaksch and P. Zoller, Ann. Phys. (NY) **315**, 52 (2005).
[5] O. Morsch and M. Oberthaler, Rev. Mod. Phys. **78**, 179 (2006).
[6] M. Greiner, O. Mandel, T. Esslinger, T. W. Hänsch, and I. Bloch, Nature (London) **415**, 39 (2002).
[7] O. Mandel, M. Greiner, A. Wldera, T. Rom, T. W. Hänsch, and I. Bloch, Nature (London) **425**, 937 (2003).
[8] T. Stöferle, H. Moritz, C. Schori, M. Köhl, and T. Esslinger, Phys. Rev. Lett. **92**, 130403 (2004).
[9] B. Paredes, A. Widera, V. Murg, O. Mandel, S. Fölling, I. Cirac, G. V. Shlyapnikov, T. W. Hänsch, and I. Bloch, Nature (London) **429**, 277 (2004).
[10] S. Fölling, F. Gerbier, A. Widera, O. Mandel, T. Gericke, and I. Bloch, Nature (London) **434**, 481 (2005).
[11] F. Gerbier, A. Widera, S. Fölling, O. Mandel, T. Gericke, and I. Bloch, Phys. Rev. Lett. **95**, 050404 (2005).
[12] F. Gerbier, S. Fölling, A. Widera, O. Mandel, and I. Bloch, Phys. Rev. Lett. **96**, 090401 (2006).
[13] S. Inouye, M. R. Andrews, J. Stenger, H. -J. Miesner, D. M. Stamper-Kurn, and W. Ketterle, Nature (London) **392**, 151 (1998).
[14] M. Greiner, C. A. Regal, and D. S. Jin, Nature (London) **426**, 537 (2003).
[15] S. Jochim, M. Bartenstein, A. Altmeyer, G. Hendl, S. Riedl, C. Chin, J. H. Denschlag, and R. Grimm, Science **302**, 2101 (2003).
[16] M. W. Zwierlein, C. A. Stan, C. H. Schunck, S. M. F.

Raupach, S. Gupta, Z. Hadzibabic, and W. Ketterle, Phys. Rev. Lett. **91**, 250401 (2006).
[17] C. A. Regal, M. Greiner, and D. S. Jin, Phys. Rev. Lett. **92**, 040403 (2004).
[18] M. W. Zwierlein, C. A. Stan, C. H. Schunck, S. M. F. Raupach, A. J. Kerman, and W. Ketterle, Phys. Rev. Lett. **92**, 120403 (2004).
[19] M. Bartenstein, A. Altmeyer, S. Riedl, S. Jochim, C. Chin, J. H. Denschlag, and R. Grimm, Phys. Rev. Lett. **92**, 120401 (2004).
[20] T. Bourdel, L. Khaykovich, J. Cubizolles, J. Zhang, F. Chevy, M. Teichmann, L. Tarruell, S. J. J. M. F. Kokkelmans, and C. Salomon, Phys. Rev. Lett. **93**, 050401 (2004).
[21] M. Rigol, A. Muramatsu, G. G. Batrouni, and R. T. Scalettar, Phys. Rev. Lett. **91**, 130403 (2003).
[22] M. Rigol and A. Muramatsu, Phys. Rev. A **69**, 053612 (2004).
[23] M. Machida, S. Yamada, Y. Ohashi, and H. Matsumoto, Phys. Rev. Lett. **93**, 200402 (2004); M. Rigol, S. R. Manmana, A. Muramatsu, R. T. Scalettar, R. R. P. Singh, and S. Wessel, Phys. Rev. Lett. **95**, 218901 (2005); M. Machida, S. Yamada, Y. Ohashi, and H. Matsumoto, Phys. Rev. Lett. **95**, 218902 (2005).
[24] X.-J. Liu, P. D. Drummond, and H. Hu, Phys. Rev. Lett. **94**, 136406 (2005).
[25] V. L. Campo, Jr. and K. Capelle, Phys. Rev. A **72**, 061602(R) (2005).
[26] X. Gao, M. Polini, M. P. Tosi, V. L. Campo, Jr., K. Capelle, and M. Rigol, Phys. Rev. B **73**, 165120 (2006).
[27] G. Modugno, F. Ferlaino, R. Heidemann, G. Roati, and M. Inguscio, Phys. Rev. A **68**, 011601(R) (2003).
[28] H. Ott, E. de Mirandes, F. Ferlaino, G. Roati, G. Modugno, and M. Inguscio, Phys. Rev. Lett. **92**, 160601 (2004).
[29] M. Köhl, H. Moritz, T. Stöferle, K. Günter, and T. Esslinger, Phys. Rev. Lett. **94**, 080403 (2005).
[30] T. Stöferle, H. Moritz, K. Günter, M. Köhl, and T. Esslinger, Phys. Rev. Lett. **96**, 030401 (2006).
[31] S. Peil, J. V. Porto, B. L. Tolra, J. M. Obrecht, B. E. King, M. Subbotin, S. L. Rolston, and W. D. Phillips, Phys. Rev. A **67**, 051603(R) (2003).
[32] J. Hubbard and J. B. Torrance, Phys. Rev. Lett. **47**, 1750 (1981).
[33] N. Nagaosa and J. Takimoto, J. Phys. Soc. Jpn. **55**, 2735 (1986).
[34] T. Egami, S. Ishihara and M. Tachiki, Science **261**, 1307 (1993).
[35] S. Ishihara, T. Egami and M. Tachiki, Phys. Rev. B **49**, 8944 (1994).
[36] R. Resta and S. Sorella, Phys. Rev. Lett. **74**, 4738 (1995); **82**, 370 (1999).
[37] M. Tsuchiizu and Y. Suzumura, J. Phys. Soc. Jpn. **68**, 3966 (1999).
[38] M. Fabrizio, A. O. Gogolin, and A. A. Nersesyan, Phys. Rev. Lett. **83**, 2014 (1999).
[39] T. Wilkens and R. M. Martin, Phys. Rev. B **63**, 235108 (2001).
[40] M. E. Torio, A. A. Aligia, and H. A. Ceccatto, Phys. Rev. B **64**, 121105 (2001).
[41] Y. Takada and M. Kido, J. Phys. Soc. Jpn. **70**, 21 (2001).
[42] J. Lou, S. Qin, T. Xiang, C. Chen, G.-S. Tian, and Z. Su, Phys. Rev. B **68**, 045110 (2003).
[43] Y. Z. Zhang, C. Q. Wu, and H. Q. Lin, Phys. Rev. B **67**, 205109 (2003).
[44] A. P. Kampf, M. Sekania, G. I. Japaridze, and P. Brune, J. Phys.: Condens. Matter **15**, 5895 (2003).
[45] S. R. Manmana, V. Meden, R. M. Noack, and K. Schönhammer, Phys. Rev. B **70**, 155115 (2004).
[46] H. Otsuka and M. Nakamura, Phys. Rev. B **71**, 155105 (2005).
[47] B. Paredes, C. Tejedor and J. I. Cirac, Phys. Rev. A **71**, 63608 (2005).
[48] G. G. Batrouni, V. Rousseau, R. T. Scalettar, M. Rigol, A. Muramatsu, P. J. H. Denteneer, and M. Troyer, Phys. Rev. Lett. **89**, 117203 (2002).
[49] V. A. Kashurnikov, N. V. Prokof'ev, and B. V. Svistunov, Phys. Rev. A **66**, 031601(R) (2002).
[50] S. Wessel, F. Alet, M. Troyer, and G. G. Batrouni, Phys. Rev. A **70**, 053615 (2004).
[51] S. R. White, Phys. Rev. Lett. **69**, 2863 (1992)
[52] U. Schollwöck, Rev. Mod. Phys. **77**, 259 (2005).